

Alamethicin I (II)	Ac-Aib-Pro-Aib-Ala-Aib-Ala (Aib)-Gln-Aib-Val-Aib-Gly-Leu-Aib-Pro-Val-Aib-Aib-Glu-Gln-Phol.
Emerimicin III (IV)	Ac-Phe-Aib-Aib-Aib-Val-Gly-Leu-Aib-Aib-Hyp-Gln-D-Iva-Hyp-Ala (Aib)-Phol.
Antiamoebin I (II)	Ac-Phe-Aib-Aib-Aib-D-Iva-Gly-Leu-Aib-Aib-Hyp-Gln-D-Iva-Hyp(Pro)-Aib-Pro-Phol.
Zervamicin IIA (II B)	Ac-Trp-Ile-Gln-Aib (Iva)-Ile-Thr-Aib-Leu-Aib-Hyp-Gln-Aib-Hyp-Aib-Pro-Phol.

Fig. 1. Sequences of some Aib-containing membrane-modifying peptides.

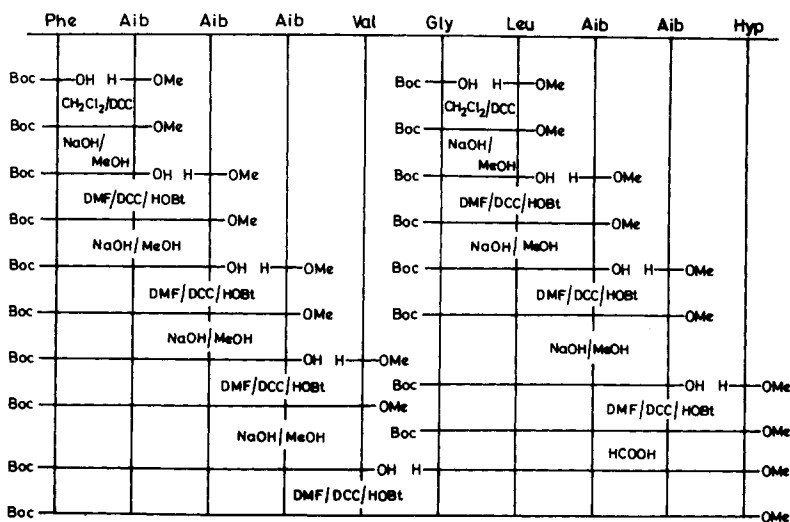


Fig. 2. The scheme for the synthesis of the peptides Boc-Phe-(Aib)₃-Val-OMe (E_{1,5}), Boc-Gly-Leu-Aib-Aib-Hyp-OMe (E_{6,10}), and Boc-Phe-(Aib)₃-Val-Gly-Leu-Aib-Aib-Hyp-OMe (E_{1,10}).

phosphorylation. A systematic investigation of the solution conformation of these peptides using 270-MHz ¹H-nmr and ir studies is also described. The results establish highly folded helical conformations for these fragments, with appreciable uncoupling activity detected for peptides having a chain length greater than seven residues.

EXPERIMENTAL

Figure 2 illustrates the scheme adopted for the synthesis of 1-5 (E_{1,5}), 6-10 (E_{6,10}), and 1-10 (E_{1,10}) emerimicin fragments. The peptides E_{1,6} (Boc-Phe-Aib-Aib-Aib-Val-Gly-OMe), E_{1,7} (Boc-Phe-Aib-Aib-Aib-Val-Gly-Leu-OMe), E_{1,8} (Boc-Phe-Aib-Aib-Aib-Val-Gly-Leu-Aib-OMe), and E_{1,9} (Boc-Phe-Aib-Aib-Aib-Val-Gly-Leu-Aib-Aib-OMe) were obtained by coupling Gly-OMe, Gly-Leu-OMe, Gly-Leu-Aib-OMe, and Gly-Leu-Aib-Aib-OMe to the free acid of peptide E_{1,5}, respectively. The coupling and work-up procedures are similar to those described earlier for model Aib peptides and have been described in detail elsewhere.^{19,20} The peptides were purified by silica gel column chromatography and checked for homogeneity by high performance liquid chromatography (HPLC) on a reverse-phase RP-18 Lichrosorb column, using

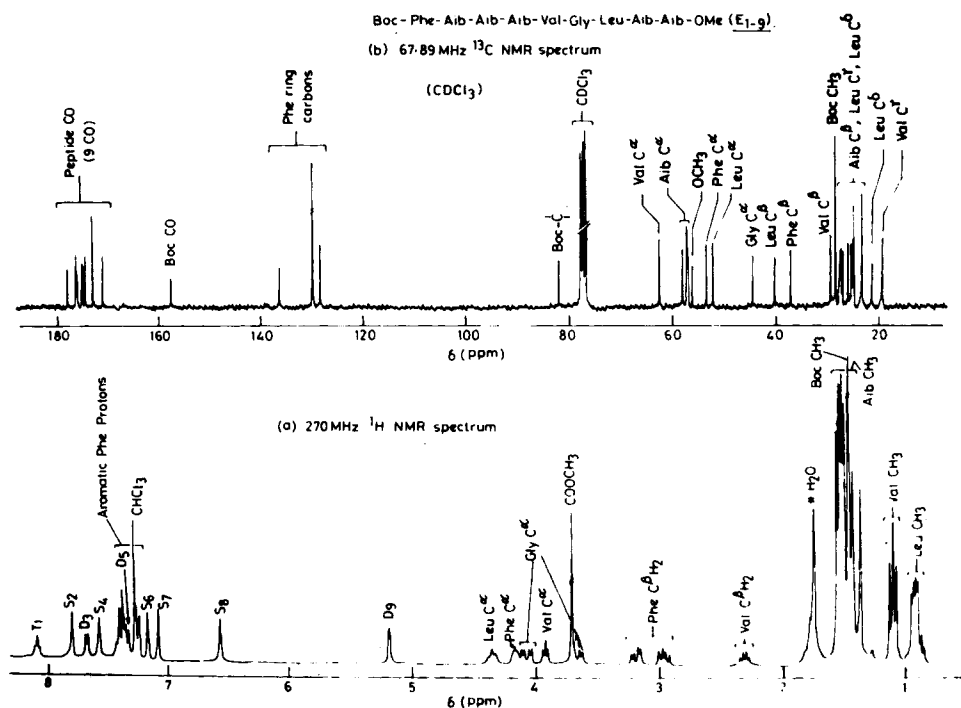


Fig. 3. (a) ^1H -nmr (270-MHz) spectrum and (b) ^{13}C -nmr (67.89-MHz) of E_{1-9} in CDCl_3 . Relevant ^{13}C chemical shifts (δ , ppm downfield from tetramethylsilane) are CO 178.2, 176.6, 176.2, 175.2, 175.0, 174.6, 173.0, (2C), 157.6 (Boc CO); Phe C_1 136.4, C_2, C_6 130.0, C_3, C_5 , 128.4; Boc C 82.0; Val C^α 62.4; Aib C^α , OCH_3 , 58.4, 57.6–56.8 (6C); Phe C^α 53.4; Leu C^α 52.2; Gly C^α 44.6; Leu C^β , 40.4; Phe C^β , 37.2; Val C^β , 29.6; Boc CH_3 (3C) 28.8; Aib C^β , Leu C^γ (11C) 28.0 – 25.0; Leu C^δ , Val C^γ (4C) 23.6, 21.6, 19.2.

methanol–water linear gradient elution, employing an LKB HPLC system (70–95% MeOH in 25 min, flow rate 0.8 mL min^{-1}). Peptides were fully characterized by amino acid analysis, 270-MHz ^1H - and 67.89-MHz ^{13}C -nmr spectra. Representative spectra for the nonpeptide E_{1-9} are illustrated in Fig. 3. Table I summarizes the relevant analytical data for the synthetic fragments. HPLC analysis and ^{13}C -nmr data established the absence of diastereomeric peptide contaminants in the purified products.

^1H -nmr spectra were recorded on a Bruker WH-270 Fourier transform nmr spectrometer, equipped with an Aspect 2000 computer at the Sophisticated Instruments Facility, Indian Institute of Science, Bangalore. In the difference nuclear Overhauser effect (NOE) experiments, the perturbed and normal spectra recorded sequentially (one on-resonance and one off-resonance) in different parts of the memory (8K of each) were obtained by low-power on-resonance saturation of a peak and by off-resonance shifting of the irradiation frequency, respectively.²¹ About 128 transients were accumulated with a relaxation delay of 3 s between transients to facilitate buildup of initial magnetization. Delineation of hydrogen-bonded NH groups was carried out as described earlier.²²

Peptide effects on respiration of rat liver mitochondria were monitored with a Hansatech oxygen electrode as described earlier.²³

TABLE I
Analytical Data for Emerimicin Fragments

Peptide ^a	Amino Acid Analysis ^b						Melting Point (°C)	HPLC Retention Time (min) ^c
	Phe	Aib	Val	Gly	Leu	Hyp		
E ₁₋₅	1.0 (1)	2.92 (3)	1.1 (1)	—	—	—	147	14.3
E ₆₋₁₀	—	2.0 (2)	—	1.1 (1)	1.0 (1)	0.92 (1)	76	6.7
E ₁₋₆	0.98 (1)	3.02 (3)	1.0 (1)	1.0 (1)	—	—	163	13.9
E ₁₋₇	0.87 (1)	3.15 (3)	0.94 (1)	1.1 (1)	0.97 (1)	—	83	18.6
E ₁₋₈	0.99 (1)	3.96 (4)	1.0 (1)	1.04 (1)	1.0 (1)	—	112	19.8
E ₁₋₉	0.98 (1)	4.95 (5)	1.0 (1)	1.05 (1)	1.02 (1)	—	125	20.7
E ₁₋₁₀	0.97 (1)	5.0 (5)	0.98 (1)	1.03 (1)	1.02 (1)	0.83 (1)	201	19.3

^a Peptides are E₁₋₅, Boc-Phe-Aib-Aib-Val-OMe; E₆₋₁₀, Boc-Gly-Leu-Aib-Aib-Hyp-OMe; E₁₋₆, Boc-Phe-Aib-Aib-Val-Gly-OMe; E₁₋₇, Boc-Phe-Aib-Aib-Val-Gly-Leu-OMe; E₁₋₈, Boc-Phe-Aib-Aib-Val-Gly-Leu-Aib-OMe; E₁₋₉, Boc-Phe-Aib-Aib-Val-Gly-Leu-Aib-OMe; E₁₋₁₀, Boc-Phe-Aib-Aib-Val-Gly-Leu-Aib-Hyp-OMe.

^b Values in parentheses are based on the sequence.

^c HPLC retention times were determined using a methanol-water gradient of 70–95% MeOH in 25 min. Flow rate 0.8 mL min⁻¹.

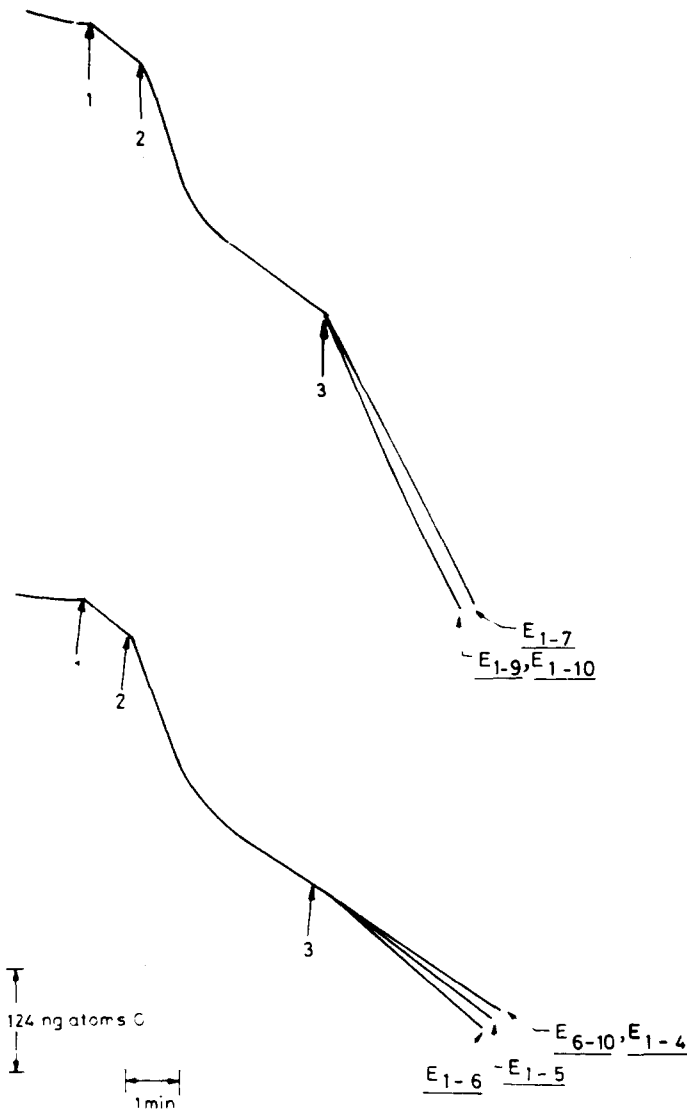


Fig. 4. Effect of synthetic fragments of emerimicin on state 4 respiration in rat liver mitochondria. Points 1, 2, and 3 indicate addition of succinate (7.5 mM), ADP (127 μ M), and peptide (50 μ M), respectively.

RESULTS AND DISCUSSION

Mitochondrial Uncoupling Activity

Figure 4 shows the effect of addition of the various emerimicin fragments on the rate of oxygen consumption by state 4 mitochondria. The peptides are compared at a concentration of 50 μ M. A minimum length of seven residues is essential for the peptide to stimulate state 4 respiration in mitochondria. The shorter fragments up to a chain length of six residues did not appreciably stimulate state 4 respiration. Addition of the longer amino terminal fragments

from heptapeptide to decapeptide did result in a significant increase in the rate of oxygen consumption, suggesting that these peptides do exhibit some uncoupling effect. The activity appears to increase with increasing chain length, with the exception of peptide E_{1-10} .

The dependence of the extent of uncoupling on the peptide concentration was assayed for each fragment and the $\phi_{1/2}$ value (concentration for half-maximal activity per milligram of mitochondrial protein) was computed from the double reciprocal plots of $[\text{peptide}]^{-1}$ vs % decrease in respiratory control index⁻¹. The $\phi_{1/2}$ values are (nmoles per mg protein) E_{1-7} 69, E_{1-8} 33.3, E_{1-9} 5.0, and E_{1-10} 35.7. These $\phi_{1/2}$ values establish that the effectiveness of the peptides as mitochondrial uncouplers increases with the chain length, when fragments E_{1-7} , E_{1-8} , and E_{1-9} are compared. A particularly interesting feature of the data is the anomalously low uncoupling activity observed for E_{1-10} . This observation has been confirmed by independent $\phi_{1/2}$ determinations on different mitochondrial preparations. It is interesting to speculate that the terminal Hyp residue in E_{1-10} may impede the formation of functional channels by association of appropriately positioned peptide molecules.

Conformational Studies

In all the peptides studied, the Aib NH resonances appear as singlets and are not a priori assigned to specific residues in the sequence. However, a distinction can be made after delineating hydrogen-bonded NH groups on the basis of conformational arguments, as described later. The Phe NH resonance was assigned to the doublet resonance at high field (urethane NH). The Gly NH was assigned to the lone triplet resonance. The Val NH was assigned by spin-decoupling experiments, establishing the $\text{NH} \leftrightarrow \text{C}^\alpha\text{H} \leftrightarrow \text{C}^\beta\text{H}$ (2.3–2.6 δ) connectivity. The remaining doublet resonance has been assigned to the Leu NH. These assignments were made in CDCl_3 solution. The corresponding assignments in $(\text{CD}_3)_2\text{SO}$ were based on solvent titration experiments, in which spectra were recorded in CDCl_3 - $(\text{CD}_3)_2\text{SO}$ mixtures. In these peptides, NH resonances were labeled as S_n (singlets), D_n (doublets), and T_n (triplets), where the subscript "n" refers to the order of appearance from low field in CDCl_3 . Although the Aib NH resonances were not assigned to individual residues, ¹H-nmr results allowed deductions about molecular conformation. The chemical shifts of the various NH resonances in peptides E_{1-5} , E_{6-10} , E_{1-6} , E_{1-7} , E_{1-8} , E_{1-9} , and E_{1-10} are summarized in Tables II–V.

Solvent accessibility of NH groups was probed using temperature dependence of chemical shifts in DMSO, paramagnetic radical-induced broadening in CDCl_3 , and solvent perturbation experiments in CDCl_3 / $(\text{CD}_3)_2\text{SO}$ mixtures.^{24,25} The results of representative experiments for the decapeptide E_{1-10} are summarized in Figs. 5 and 6. The $d\delta/dT$ values for the various peptides studied are listed in Tables II–V. In all cases strongly solvent-shielded NH groups are characterized by $d\delta/dT$ values ≤ 0.003 ppm/K, $\Delta\delta(\delta_{(\text{CD}_3)_2\text{SO}} - \delta_{\text{CDCl}_3})$ values < 0.5 ppm, and relatively little broadening in the presence of the paramagnetic radical TEMPO. In all the peptides the first two amino terminal residues are invariably characterized as fully exposed to the solvent by these criteria. For the amino terminal fragments E_{1-5} to E_{1-10} the two exposed NH resonances can be assigned to Phe(1) and Aib(2) NH, while for

TABLE II
¹H-NMR Parameters^a

NH Resonances ^b	Boc-Phe-Aib-Aib-Aib-Val-OMe (E ₁₋₅)			Boc-Gly-Leu-Aib-Aib-Hyp-OMe (E _{6,10})			
	δ (ppm) CDCl ₃	δ (ppm) (CD ₃) ₂ SO	dδ/dT (ppm/K) (CD ₃) ₂ SO	NH Resonances ^b	δ (ppm) CDCl ₃	δ (ppm) (CD ₃) ₂ SO	dδ/dT (ppm/K) (CD ₃) ₂ SO
D ₁ (Val NH) ^c	7.48	7.46	0.0024	S ₁ [Aib(4) NH]	7.29	7.33	0.0016
S ₂ [Aib(4) NH]	7.31	7.44	0.0026	D ₂ (Leu NH)	7.20	8.01	0.0050
S ₃ [Aib(3) NH]	7.16	7.43	0.0034	S ₃ [Aib(3) NH]	7.09	8.22	0.0062
S ₄ [Aib(2) NH]	6.32	8.43	0.0042	T ₄ (Gly NH)	5.72	6.94	0.0048
D ₆ (Phe NH) ^c	5.10	7.11	0.0082				

^aPeptide concentration: ~ 10 mM.

^bAib NH resonances have been assigned tentatively.

^cJ_{HNC-H} (Hz) values are E₁₋₅, Val NH, 8.0 (CDCl₃), 6.5 [(CD₃)₂SO]; Phe NH, 4.4 (CDCl₃), 5.1 [(CD₃)₂SO]. E_{6,10}, Leu NH, 5.1 (CDCl₃), 5.8 [(CD₃)₂SO].

TABLE III
¹H-NMR Parameters^a

NH Resonances ^b	Boc-Phe-Aib-Aib-Val-Gly-OMe (E ₁₋₆)			Boc-Phe-Aib-Aib-Val-Gly-Leu-OMe (E ₁₋₇)			
	δ (ppm) CDCl ₃	δ (ppm) (CD ₃) ₂ SO	dδ/dT (ppm/K) (CD ₃) ₂ SO	NH Resonances ^b	δ (ppm) CDCl ₃	δ (ppm) (CD ₃) ₂ SO	dδ/dT (ppm/K) (CD ₃) ₂ SO
T ₁ (Gly NH)	7.85	7.87	0.0032	T ₁ (Gly NH)	7.95	7.79	0.0016
S ₂ (Aib NH)	7.62	7.69	0.0035	S ₂ [Aib(3) NH]	7.68	7.81	0.0042
D ₃ (Val NH) ^c	7.35	7.33	0.0020	S ₃ [Aib(4) NH]	7.47	7.70	0.0028
S ₄ (Aib NH)	7.30	7.65	0.0030	D ₄ (Val NH) ^c	7.32	7.69	0.0035
S ₅ [Aib(2) NH]	6.46	8.41	0.0058	D ₅ (Leu NH) ^c	7.09	7.26	0.0011
D ₆ (Phe NH) ^c	5.05	7.06	0.0068	S ₆ [Aib(2) NH]	6.52	8.48	0.0064
				D ₇ (Phe NH) ^c	5.10	7.06	0.0066

^a Peptide concentration: ~ 10 mM.

^b Assignments of Aib NH resonances are tentative.

^c $J_{\text{HNC}^{\alpha}\text{H}}$ values (Hz) are E₁₋₆, Val NH, 7.7 (CDCl₃), 6.5 [(CD₃)₂SO]; Phe NH, 7.3 [(CD₃)₂SO]. E₁₋₇, Val NH, 7.3 (CDCl₃), 7.3 [(CD₃)₂SO]; Leu NH 8.7 (CDCl₃), 8.5 [(CD₃)₂SO]; Phe NH 7.0 [(CD₃)₂SO].

TABLE IV
¹H-NMR Parameters

Boc-Phe-Aib-Aib-Aib-Val-Gly-Leu-Aib-OMe (E _{1,9}) ^a			Boc-Phe-Aib-Aib-Aib-Val-Gly-Leu-Aib-Aib-OMe (E _{1,9}) ^b				
NH Resonances ^c	δ (ppm) CDCl ₃	δ (ppm) (CD ₃) ₂ SO	dδ/dT (ppm/K) (CD ₃) ₂ SO	NH Resonances ^c	δ (ppm) CDCl ₃	δ (ppm) (CD ₃) ₂ SO	dδ/dT (ppm/K) (CD ₃) ₂ SO
T ₁ (Gly NH)	8.06	7.80	0.0018	T ₁ (Gly NH)	8.08	7.87	0.0020
S ₂ (Aib NH)	7.74	7.80	0.0030	S ₂ (Aib NH)	7.79	7.84	0.0034
D ₃ (Val NH) ^d	7.56	7.53	0.0035	D ₃ (Val NH) ^d	7.67	7.61	0.0035
S ₄ [Aib(3) NH]	7.52	7.94	0.0066	S ₄ [Aib(3) NH]	7.56	7.85	0.0054
S ₅ (Aib NH)	7.40	7.70	0.0024	D ₅ (Leu NH) ^d	7.32	7.42	0.0008
D ₆ (Leu NH) ^d	7.34	7.41	0.0014	S ₆ (Aib NH)	7.16	7.72	0.0022
S ₇ [Aib(2) NH]	6.53	8.47	0.0064	S ₇ (Aib NH)	7.07	7.23	0.0020
D ₈ (Phe NH) ^d	5.11	7.05	0.0064	S ₈ [Aib(2) NH]	6.56	8.49	0.0062
				D ₉ (Phe NH) ^d	5.17	7.05	0.0064

^a Peptide concentration: ~ 8 mM.

^b Peptide concentration: ~ 5 mM.

^c All the Aib residues could not be assigned.

^d ^J_{HNC^αH} values (Hz) are E_{1,6}, Val NH, 5.9 (CDCl₃), 8.7 [(CD₃)₂SO]; Leu NH, 8.7 (CDCl₃), 8.0 [(CD₃)₂SO], Phe NH 8.1 [(CD₃)₂SO]. E_{1,9}, Val NH 5.8 (CDCl₃), 6.3 [(CD₃)₂SO]; Leu NH 5.1 (CDCl₃), 7.3 [(CD₃)₂SO]; Phe NH 7.3 [(CD₃)₂SO].

TABLE V
¹H-NMR Parameters^a for Boc-Phe-Aib-Aib-Aib-Val-Gly-Leu-Aib-Aib-Hyp-OMe (E₁₋₁₀)

NH Resonances ^b	δ (ppm) CDCl ₃	δ (ppm) (CD ₃) ₂ SO	$d\delta/dT$ (ppm/K)
T ₁ (Gly NH)	8.08	7.90	0.0010
S ₂ (Aib NH)	7.91	7.83	0.0034
D ₃ (Val NH) ^c	7.70	7.56	0.0032
S ₄ [Aib(3) NH]	7.69	7.78	0.0048
D ₅ (Leu NH) ^c	7.32	7.47	0.0014
S ₆ (Aib NH)	7.30	7.74	0.0022
S ₇ (Aib NH)	7.19	7.24	0.0018
S ₈ [Aib(2) NH]	7.13	8.56	0.0062
D ₉ (Phe NH) ^c	5.82	7.05	0.0050

^a Peptide concentration: ~ 5 mM.

^b Aib resonances, wherever mentioned, are tentatively assigned.

^c $J_{\text{HNC}^{\alpha}\text{H}}$ values (Hz) are Val NH, 6.3 (CDCl₃), 5.8 [(CD₃)₂SO]; Leu NH 7.7 [(CD₃)₂SO]; Phe NH, 8.0 [(CD₃)₂SO].

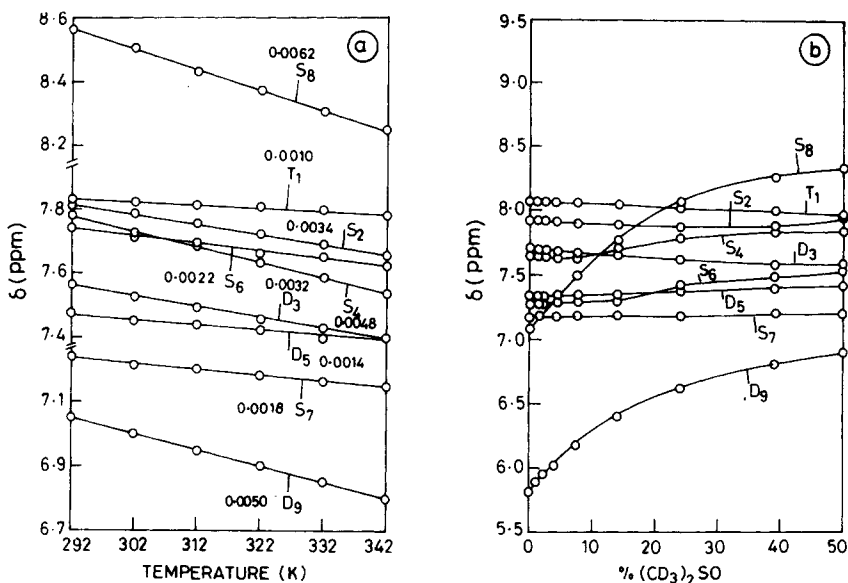


Fig. 5. (a) Temperature dependence of NH proton chemical shifts of the peptide Boc-Phe-(Aib)₃-Val-Gly-Leu-Aib-Aib-Hyp-OMe (E₁₋₁₀) in (CD₃)₂SO. (b) Solvent dependence of NH proton chemical shifts of the peptide E₁₋₁₀ in CDCl₃-(CD₃)₂SO mixtures. S_n, D_n, and T_n refer to singlet, doublet and triplet resonances. The subscript "n" refers to the order of appearance from low field in CDCl₃. $d\delta/dT$ values for the NH protons are indicated against the traces in (a).

E₆₋₁₀, the Gly(1) and Leu(2) NH groups are solvent exposed. From the assignments in Tables II-V, it can be seen that in the peptides E₁₋₅ and E₁₋₆ one of the Aib NH groups has an intermediate $d\delta/dT$ value of 0.0035 ppm/K, although the $\Delta\delta$ values are small. In E₁₋₇ one Aib NH [tentatively assigned to Aib(3) NH] and Val(5) NH have moderate $d\delta/dT$ values. In E₁₋₈ and E₁₋₉ one additional Aib NH assigned to Aib(3) NH is clearly solvent exposed, as evidenced by its high $d\delta/dT$ value. Furthermore, the Val(5) NH

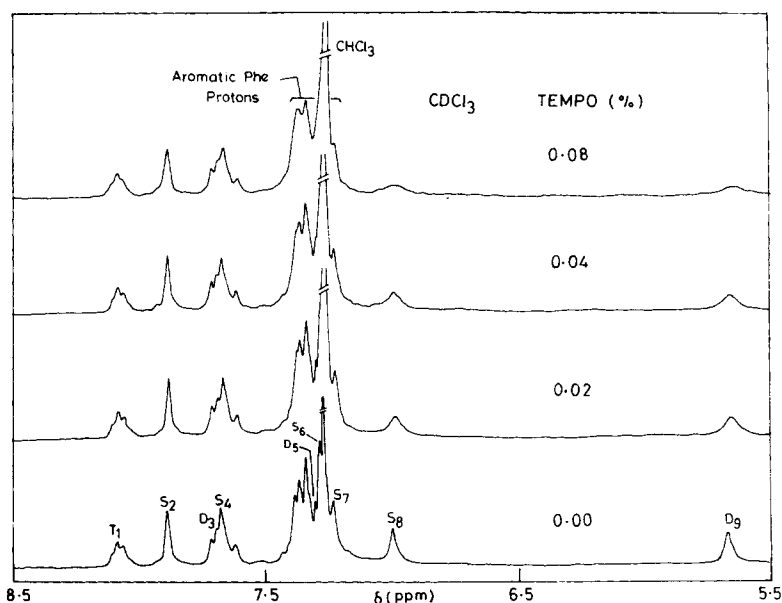


Fig. 6. Partial 270-MHz ^1H -nmr spectra of NH resonances in CDCl_3 as a function of TEMPO concentration. The individual resonances are indicated as in Fig. 5.

in both these peptides is only moderately shielded. In E_{1-10} one Aib NH appears appreciably solvent exposed in addition to the two amino terminal NH groups. The number of strongly (partially) shielded NH groups in $(\text{CD}_3)_2\text{SO}$ in the various peptides are E_{1-5} 2(1), E_{6-10} 1, E_{1-6} 3(1), E_{1-7} 3(1), E_{1-8} 4(1) and E_{1-9} 4(2), and E_{1-10} 4(2). These estimates are based on the $d\delta/dT$ values.

In CDCl_3 , only two NH groups corresponding to residues 1 and 2 appear solvent exposed. These resonances show appreciable shifts on addition of strongly hydrogen bond accepting solvents like $(\text{CD}_3)_2\text{SO}$ up to a concentration of 20 volume percent in CDCl_3 solutions. Furthermore, these resonances also broaden considerably relative to the remaining NH resonances on addition of the paramagnetic radical. The nmr results thus suggest small differences in the conformations of the peptides in CDCl_3 and $(\text{CD}_3)_2\text{SO}$, with a greater number of solvent-shielded NH groups in the former. In nmr studies of similar acyclic peptides, solvent-shielded NH resonances have almost invariably been assigned to intramolecularly hydrogen-bonded NH groups.^{22, 26-29}

The $J_{\text{HNC}^\alpha\text{H}}$ values for the L-amino acid residues in the various peptides are listed in footnotes to Tables II-V. The Phe(1) NH has a low value (< 5 Hz) in CDCl_3 in all the peptides and is in fact, a broad unresolved doublet resonance in sequences longer than E_{1-5} . The $J_{\text{HNC}^\alpha\text{H}}$ values in $(\text{CD}_3)_2\text{SO}$ are somewhat larger for Phe(1) NH. The $J_{\text{HNC}^\alpha\text{H}}$ value in CDCl_3 for Val NH is < 8 Hz in all peptides except E_{1-5} , where this is the C-terminal residue. The changes when going to $(\text{CD}_3)_2\text{SO}$ are very small except in the case of E_{1-8} . For Leu NH, large $J_{\text{HNC}^\alpha\text{H}}$ values (> 8 Hz) are observed for E_{1-7} and E_{1-8} . Helical conformations will generally be characterized by low $J_{\text{HNC}^\alpha\text{H}}$ values (< 5 Hz) and more extended structures by large values (> 8 Hz).³⁰ The limited number

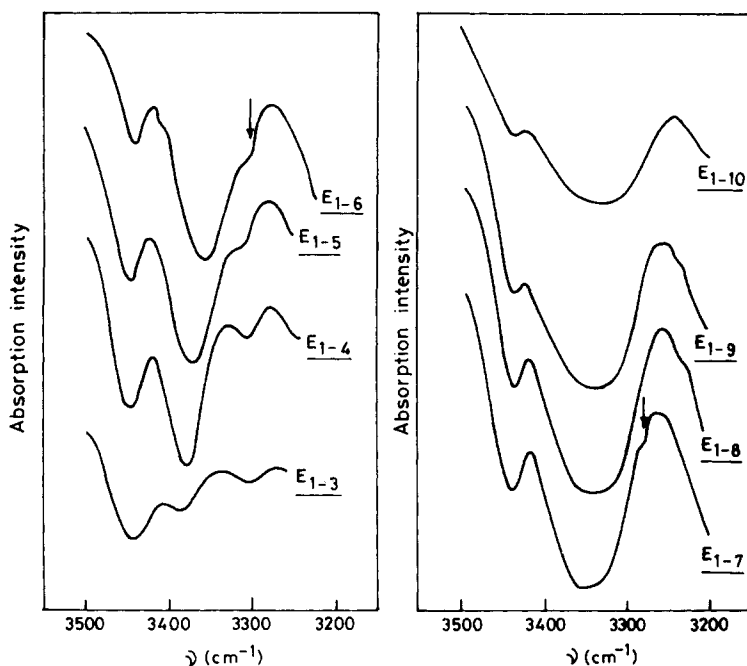


Fig. 7. Infrared spectra (NH-stretching bands) of synthetic emerimicin fragments in CHCl_3 solutions at $2 \times 10^{-4}M$. The arrows indicate the position of the solvent absorption band.

of non-Aib residues in these sequences, and their positioning near or at the chain termini in several peptide fragments, precludes a more detailed analysis of the conformations based on $J_{\text{HNC}^{\alpha}\text{H}}$ values. Indeed, as noted later, the possibility of interconversions between helical conformations of opposite handedness can lead to dynamic averaging of J values. The nmr data in CDCl_3 may also be influenced by peptide association.³¹⁻³³ However, as noted earlier for helical Aib-containing sequences, aggregation does not perturb intramolecular hydrogen-bonding patterns but occurs through the mediation of solvent-exposed NH groups.^{32,33}

Infrared studies can be used to directly estimate the extent of intramolecular hydrogen bonding.³⁴ The NH stretching regions of the ir spectra of the N-terminal fragments of emerimicin III and IV with increasing chain length from tripeptide to decapeptide in chloroform solution, at the concentration $2 \times 10^{-4}M$, are shown in Fig. 7. At this concentration it is generally assumed that only intramolecular hydrogen bonds are predominant.³⁴⁻³⁷ Under identical conditions all N-terminal fragments from tripeptide to decapeptide exhibit two NH-stretching bands at $3440\text{--}3445\text{ cm}^{-1}$ and at $3330\text{--}3380\text{ cm}^{-1}$ (Fig. 7) characteristic of free [$\nu_{\text{NH}}(\text{f})$] and hydrogen-bonded [$\nu_{\text{NH}}(\text{hb})$] stretching frequencies, respectively. The lower frequency band at $3330\text{--}3380\text{ cm}^{-1}$ observed in these peptides at the concentration $2 \times 10^{-4}M$ may be assigned to intramolecularly hydrogen-bonded NH groups.

A plot of the ratio of the intensities of the bands [$\nu_{\text{NH}}(\text{hb})/\nu_{\text{NH}}(\text{f})$] as a function of chain length increases regularly from tripeptide to nonapeptide (Fig. 8). This suggests that an increase in the chain length accompanied by an increase in the number of NH groups leads to the folding of the peptide

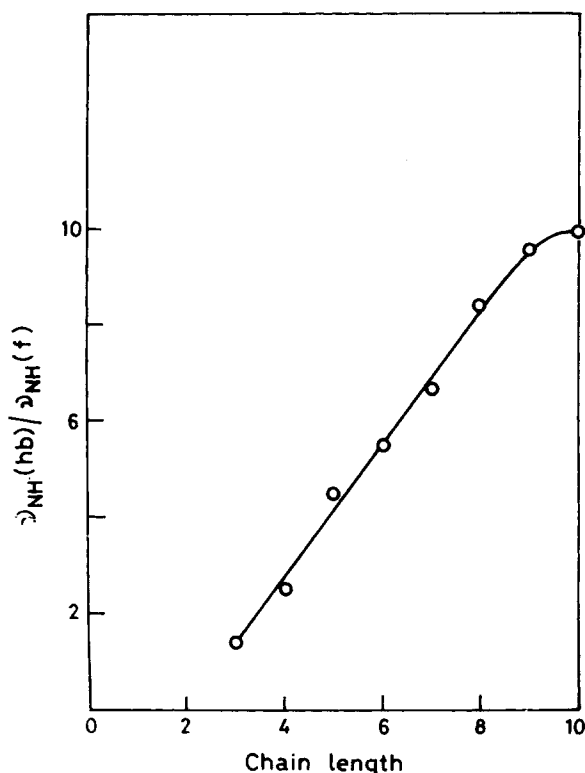


Fig. 8. A plot of the ratio of the intensities of the NH-stretching bands [$\nu_{\text{NH}}(\text{hb})/\nu_{\text{NH}}(\text{f})$] as a function of chain length for the N-terminal fragments of emerimicin III and IV. $\nu_{\text{NH}}(\text{f})$, 3440–3445 cm^{-1} and $\nu_{\text{NH}}(\text{hb})$, 3330–3380 cm^{-1} .

backbone, with an increase in the number of intramolecularly hydrogen-bonded NH groups. Similar results have been obtained for homooligopeptides of Aib(Z(Aib) $_n$ OtBu $n = 3, 4, 5$)³⁶ and amino terminal alamethicin fragments.³⁵ There is not much difference in the ratio [$\nu_{\text{NH}}(\text{hb})/\nu_{\text{NH}}(\text{f})$] for the nonapeptide E₁₋₉ and the decapeptide E₁₋₁₀. This is reasonable, since both peptides may be expected to have the same number of hydrogen-bonded NH groups.

The intensity of the hydrogen-bonded NH-stretching band can be used to quantitatively estimate the number of intramolecularly hydrogen-bonded NH groups. ¹H-nmr studies of the tetrapeptide E₁₋₄ show the presence of two intramolecular hydrogen bonds, as reported earlier.¹⁵ The intensity of the $\nu_{\text{NH}}(\text{hb})$ band for this peptide is taken to be equivalent to two hydrogen bonds. On this basis the number of intramolecularly hydrogen-bonded NH groups as determined from the $\nu_{\text{NH}}(\text{hb})$ band intensities of these peptides are E₁₋₃ one, E₁₋₅ three, E₁₋₆ four, E₁₋₇ five, E₁₋₈ six, E₁₋₉ seven, and E₁₋₁₀ seven. Similar studies have also been reported for alamethicin fragments^{34,35} and model peptides.³⁶

Backbone Conformations

The only peptide that shows a single solvent-shielded NH group is the central pentapeptide E₆₋₁₀. Here the lone shielded NH group can be assigned

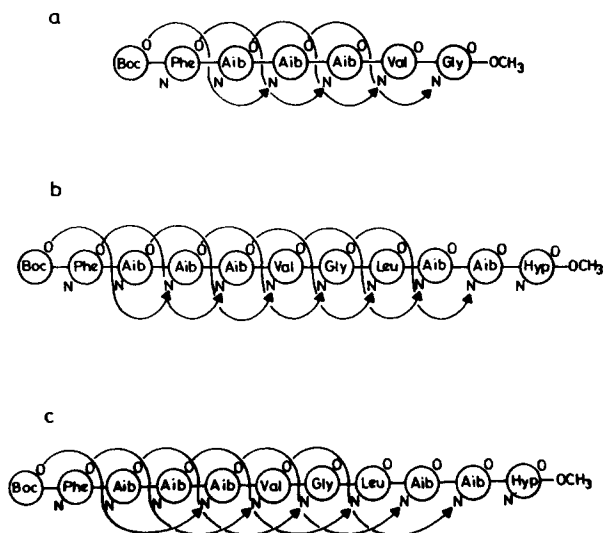


Fig. 9. Schematic hydrogen-bonding schemes proposed for peptides E_{1-6} (a) and E_{1-10} (b, c), consistent with the spectral data. (b) 3_{10} -helical conformation and (c) α -helical conformation.

to Aib(4) NH stabilizing a Leu-Aib β -turn conformation, with an intramolecular $4 \rightarrow 1$ hydrogen bond between Aib(4) NH and Gly(1) CO. This conformation may be favored because of the tendency of X-Aib sequence to adopt β -turn structures.^{4,7} For the remaining amino terminal fragments, the nmr and ir studies in chloroform indicate a progressive increase in the number of intramolecular hydrogen bonds when going from E_{1-4} to E_{1-9} . As expected, E_{1-10} and E_{1-9} appear to possess the same number of intramolecular hydrogen bonds since the C-terminal residue in the former is Hyp, which does not possess an NH group. These results are consistent with the extension of a 3_{10} -helical structure, stabilized by successive $4 \rightarrow 1$ intramolecular hydrogen bonds. Typical hydrogen-bonding patterns compatible with the spectral data in chloroform are shown in Fig. 9. The observed helical folding is fully consistent with the tendency of Aib-rich sequences to adopt 3_{10} - or α -helical conformations.^{4-7, 38-42}

A particular point of interest in the sequence of emerimicin is the presence of an L-amino acid (L-Phe) as the N-terminal residue. This raises the possibility that the amino terminal β -turn with Phe(1) and Aib(2) as the corner residues may in fact be either type II ($\phi_{\text{Phe}} \sim -60^\circ$, $\psi_{\text{Phe}} \sim +120^\circ$, $\phi_{\text{Aib}} \sim +70^\circ$, $\psi_{\text{Aib}} \sim 20^\circ$) or type III ($\phi_{\text{Phe}} = \phi_{\text{Aib}} = -60^\circ$; $\psi_{\text{Phe}} = \psi_{\text{Aib}} = -30^\circ$).⁴³ In the former case the successive β -turns must belong to the type III category,^{7,44} which would imply a left-handed helical folding of the segment following residue 2. In the latter case, a succession of type III β -turns would generate a 3_{10} -helix. A recent study of antimoebin, a fungal peptide produced by *Emericellopsis poonensis* Thirum., *Emericellopsis synnematicola* Mathur and Thirum., and *Cephalosporium pimprina* Thirum., which also possesses L-Phe-Aib as the first two residues, suggest a Type II β -turn conformation for this segment.⁴⁴ Such conformations can be readily recognized by the presence of an interresidue NOE between the Phe(1) C ^{α} H and Aib(2) NH protons.^{21,44}

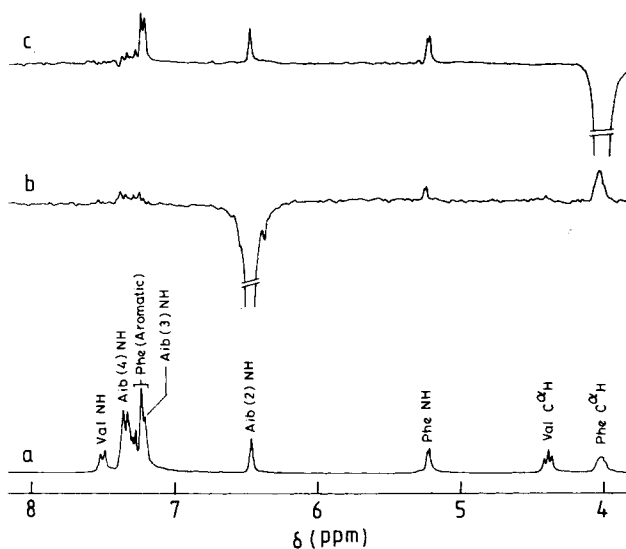


Fig. 10. (a) Partial 270-MHz ^1H -nmr spectrum of $\text{E}_{1.5}$ in CDCl_3 . (b, c) Difference NOE spectra ($\times 32$) obtained by irradiation of Aib(2) NH(b), and Phe C^αH (c) resonances.

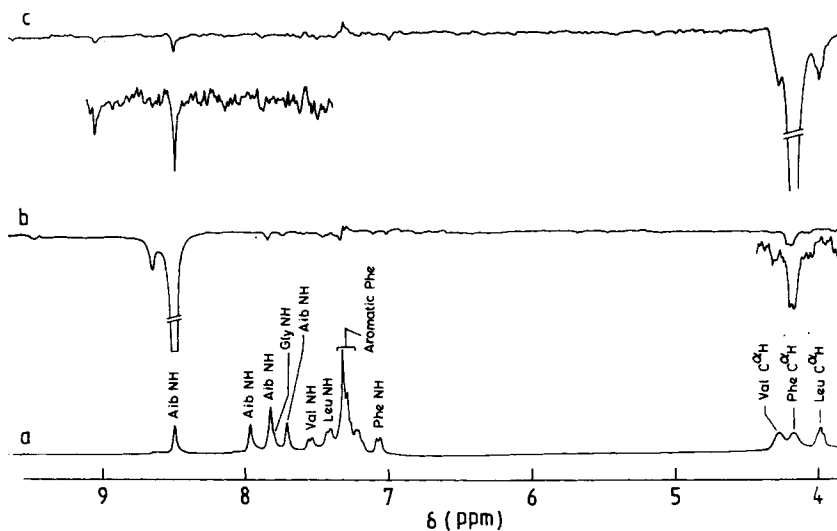


Fig. 11. (a) Partial 270-MHz ^1H -nmr spectra of $\text{E}_{1.8}$ in $(\text{CD}_3)_2\text{SO}$. (b, c) Difference NOE spectra ($\times 16$) obtained by irradiation of Aib NH(b) and Phe C^αH (c) resonances. The inset shows the Phe $\text{C}^\alpha\text{H} \leftrightarrow$ Aib NH NOE at higher magnification ($\times 64$).

The results of representative difference NOE experiments on peptides $\text{E}_{1.5}$ and $\text{E}_{1.8}$ are shown in Figs. 10 and 11. For $\text{E}_{1.5}$ in CDCl_3 , irradiation of the Phe C^αH resonance results in clear positive NOEs on the Phe NH (intraresidue) and Aib(2) NH (interresidue) protons. In addition, an NOE is also observed on the aromatic protons. Irradiation of the Aib(2) NH results in a large NOE on the Phe C^αH proton and a smaller NOE on the Phe NH proton. The Phe $\text{C}^\alpha\text{H} \leftrightarrow$ Aib(2) NH NOE is diagnostic of a ψ_{Phe} value of $\sim 120^\circ$

TABLE VI

Emerimicin Fragments	Number of Intramolecularly Hydrogen-Bonded NH Groups Determined from Spectroscopic Studies				Conformational Inference ^a	
	¹ H NMR		IR		CDCl ₃	(CD ₃) ₂ SO
	CDCl ₃	(CD ₃) ₂ SO	CDCl ₃	(CD ₃) ₂ SO		
Boc-Phe-Aib-Aib-Aib-OMe E ₁₋₄	2	2	2	2	Consecutive β-turn (III-III, III-III' or II-III')	Consecutive β-turn (III-III, III-III' or II-III')
Boc-Phe-Aib-Aib-Aib-Val-OMe E ₁₋₅	3	3	3	3	3 ₁₀	3 ₁₀
Boc-Phe-Aib-Aib-Aib-Val-Gly-OMe E ₁₋₆	4	4	4	4	3 ₁₀	3 ₁₀
Boc-Phe-Aib-Aib-Aib-Val-Gly-Leu-OMe E ₁₋₇	5	4	4	5	3 ₁₀	α or partially opened 3 ₁₀
Boc-Phe-Aib-Aib-Aib-Val-Gly-Leu-Aib-OMe E ₁₋₈	6	5	5	6	3 ₁₀	α or partially opened 3 ₁₀
Boc-Phe-Aib-Aib-Aib-Val-Gly-Leu-Aib-OMe E ₁₋₉	7	6	6	7	3 ₁₀	α or partially opened 3 ₁₀
Boc-Phe-Aib-Aib-Aib-Val-Gly-Leu-Aib-Hyp-OMe E ₁₋₁₀	7	6	6	7	3 ₁₀	α or partially opened 3 ₁₀

^a If the nucleating Phe-Aib β-turn is type II, then a succeeding helix will be left handed, whereas a right-handed helix is obtained if the Phe-Aib segment occupies the corner positions of a type III β-turn.

$\pm 30^\circ$,^{45,46} supporting a type II β -turn conformation of this segment. The Phe NH \leftrightarrow Aib(2) NH NOE ($N_{i+1}H \leftrightarrow N_{i+2}H$) is, however, not expected for the $i + 1$ and $i + 2$ residues of a type II β -turn.⁴⁵ This NH-NH NOE is, in fact, characteristic of a helical conformation or a type III β -turn.⁴⁵ The simultaneous observation of these two NOEs suggests that both conformational states are in fact populated in solution and that a rapid dynamic equilibrium exists between these structures. Indeed, the highest $d\delta/dT$ values observed for one of the Aib NH [tentatively assigned to Aib(3) NH] in DMSO in the case of the amino terminal emerimicin peptides is consistent with a degree of structural flexibility for the N-terminal β -turns. Figure 11 shows the results of typical NOE experiments on the octapeptide E_{1-8} in DMSO. In this case the observed NOEs are negative, indicating that the molecular correlation time τ_c is long enough to make $\omega\tau_c > 1$.⁴⁷ The observed Phe C $^\alpha$ H \leftrightarrow Aib(2) NH NOE is again consistent with a type II β -turn conformation for the N-terminal fragment. Interestingly, no NOE was detectable between Aib(2) NH and Phe NH protons. Table VI summarizes the results of the spectral studies on the emerimicin fragments and the conformational inferences drawn therefrom. The results of this study suggest the presence of an additional solvent-exposed NH groups in DMSO as compared to those for the longer peptides E_{1-7} , E_{1-8} , E_{1-9} , and E_{1-10} . This NH group, which may be assigned to Aib(3) NH, may be exposed either due to partial unfolding of the N-terminal β -turn or by a population of α -helical structures in which the first three N-terminal NH groups are expected to be solvent exposed. A distinction between these two possibilities does not appear possible at this time.²⁹

In considering left-handed 3_{10} -helical structures for the longer fragments E_{1-6} to E_{1-10} , it must be emphasized that such structures will necessitate positive ϕ, ψ values for L-Val and L-Leu residues. This region of conformational space is intrinsically less likely for L-residues.⁴⁸ It is noteworthy that the solvent exposure of the Aib(3) NH in the longer peptides is appreciably greater, suggesting that right-handed helical conformations may be favored at the expense of destabilizing the Phe(1)-Aib(2) β -turn. The simultaneous observation of the Phe(1) C $^\alpha$ H \leftrightarrow Aib(2) NH NOE and a high $d\delta/dT$ value of Aib(3) NH in E_{1-8} could, in fact, be rationalized in terms of a partially unfolded conformation when $\psi_{\text{Phe}} \sim 120^\circ$, but Aib(2) ϕ, ψ fall in the right-handed helical region ($\phi \sim -60^\circ, \psi \sim -30^\circ$) such that the N-terminal β -turn is disrupted.

CONCLUSIONS

The spectral studies described in this report reaffirm the overwhelming tendency of Aib residues to promote helical folding. Sequence-dependent conformational variability has also been noted, raising questions regarding the sense of helical folding and solvent effects for the Aib peptide antibiotics that possess an N-terminal L-residue. Mitochondrial uncoupling activity observed for some of these relatively short hydrophobic peptides must reflect their ability to associate in the lipid phase and alter transmembrane permeabilities. The relatively low activity observed for the peptide E_{1-10} , which possesses a terminal Hyp group, suggests that appreciable insertion of peptides into the membrane may be necessary before uncoupling activity is manifested in the case of the short sequences.

We are grateful to Professor Claudio Toniolo, University of Padova, Italy, for kindly providing the amino acid analyses, and to Mr. S. Raghobhama, Sophisticated Instruments Facility, Indian Institute of Science, Bangalore, for his help with the NOE experiments. This research was supported by a grant from the Department of Science and Technology, Government of India. P.A.R. was supported by a Teacher-Fellowship of the University Grants Commission.

References

1. Argoudelis, A. D. & Johnson, L. E. (1974) *J. Antibiot.* **27**, 274-282.
2. Pandey, R. C., Carter Cook, J., Jr. & Rinehart, K. L., Jr. (1977) *J. Am. Chem. Soc.* **99**, 5205-5206.
3. Mueller, P. & Rudin, D. O. (1968) *Nature* **217**, 713-719.
4. Nagaraj, R. & Balaram, P. (1981) *Acc. Chem. Res.* **14**, 356-362.
5. Jung, G., Brückner, H. & Schmitt, H. (1981) in *Structure and Activity of Natural Peptides*, Voelter, W. and Weitzel, G., Eds., Walter de Gruyter, Berlin, pp. 75-114.
6. Mathew, M. K. & Balaram, P. (1983) *Mol. Cell. Biochem.* **50**, 47-64.
7. Prasad, B. V. V. & Balaram, P. (1984) *CRC Crit. Revs. Biochem.* **16**, 307-348.
8. Schmitt, H. & Jung, G. (1985) *Liebigs Ann. Chem.* **1985**, 321-344.
9. Hall, J. E., Vodyanoy, I., Balasubramanian, T. M. & Marshall, G. R. (1984) *Biophys. J.* **45**, 233-247.
10. Menestrina, G., Voges, K.-P., Jung, G. & Boheim, G. (1986) *J. Membr. Biol.* **93**, 111-132.
11. Balasubramanian, T. M., Redlinski, A. S. & Marshall, G. R. (1981) in *Peptides: Synthesis Structure and Function, Proceedings of the Seventh American Peptide Symposium*, Rich, D. H. and Gross, E., Eds., Pierce Chemical Co., Rockford, IL, pp. 61-64.
12. Benedetti, E., Bavoso, A., DiBlasio, B., Pavone, V., Pedone, C., Toniolo, C. & Bonora, G. M. (1982) *Proc. Natl. Acad. Sci. USA* **79**, 7951-7954.
13. Toniolo, C., Bonora, G. M., Bavoso, A., Benedetti, E., DiBlasio, B., Pavone, V. & Pedone, C. (1985) *J. Biomol. Struct. Dynam.* **3**, 585-598.
14. Bavoso, A., Benedetti, E., DiBlasio, B., Pavone, V., Pedone, C., Toniolo, C. & Bonora, G. M. (1986) *Proc. Natl. Acad. Sci. USA* **83**, 1988b-1992.
15. Bardi, R., Piazzesi, A. M., Toniolo, C., Raj, P. A., Raghobhama, S. & Balaram, P. (1986) *Int. J. Biol. Macromol.* **8**, 201-206.
16. Toniolo, C., Bonora, G. M., Benedetti, E., Bavoso, A., DiBlasio, B., Pavone, V. & Pedone, C. (1985) *Int. J. Biol. Macromol.* **7**, 357-362.
17. Toniolo, C., Bonora, G. M., Benedetti, E., Bavoso, A., DiBlasio, B., Pavone, V. & Pedone, C. (1983) *Biopolymers* **22**, 1335-1356.
18. Nagaraj, R. & Balaram, P. (1979) *Biochem. Biophys. Res. Commun.* **89**, 1041-1049.
19. Nagaraj, R. & Balaram, P. (1981) *Tetrahedron* **37**, 2001-2005.
20. Vijayakumar, E. K. S. & Balaram, P. (1983) *Tetrahedron* **39**, 2725-2731.
21. Rao, B. N. N., Kumar, A., Balaram, H., Ravi, A. & Balaram, P. (1983) *J. Am. Chem. Soc.* **105**, 7423-7428.
22. Vijayakumar, E. K. S. & Balaram, P. (1983) *Biopolymers* **22**, 2133-2140.
23. Das, M. K., Basu, A. & Balaram, P. (1985) *Biochem. Intl.* **11**, 357-363.
24. Wüthrich, K. (1976) *NMR in Biological Research: Peptides and Proteins*, North-Holland, Amsterdam.
25. Kessler, H. (1982) *Angew. Chem. Int. Ed. Engl.* **21**, 512-523.
26. Nagaraj, R. & Balaram, P. (1981) *Biochemistry* **20**, 2828-2835.
27. Iqbal, M. & Balaram, P. (1981) *J. Am. Chem. Soc.* **103**, 5548-5552.
28. Iqbal, M. & Balaram, P. (1981) *Biochemistry* **20**, 4866-4871.
29. Balaram, H., Sukumar, M. & Balaram, P. (1986) *Biopolymers* **25**, 2209-2223.
30. Bystrov, V. F. (1976) *Prog. NMR Spectrosc.* **10**, 41-81.
31. Stevens, E. S., Sugawara, N., Bonora, G. M. & Toniolo, C. (1980) *J. Am. Chem. Soc.* **102**, 7048-7050.
32. Iqbal, M. & Balaram, P. (1981) *Biochemistry* **20**, 7278-7284.
33. Iqbal, M. & Balaram, P. (1982) *Biopolymers* **21**, 1427-1433.
34. Rao, Ch. P., Nagaraj, R., Rao, C. N. R. & Balaram, P. (1979) *FEBS Lett.* **100**, 244-248.
35. Rao, Ch., P., Nagaraj, R., Rao, C. N. R. & Balaram, P. (1980) *Biochemistry* **19**, 425-431.

36. Benedetti, E., Bavoso, A., DiBlasio, B., Pavone, V., Pedone, C., Crisma, M., Bonora, G. M. & Toniolo, C. (1982) *J. Am. Chem. Soc.* **104**, 2437-2444.
37. Toniolo, C., Bonora, G. M., Barone, V., Bavoso, A., Benedetti, E., DiBlasio, B., Grimaldi, P., Lelj, F., Pavone, V. & Pedone C. (1985) *Macromolecules* **18**, 895-902.
38. Balamam, P. (1983) in *Peptides: Structure and Function, Proceedings of the Eighth American Peptide Symposium*, Hruby, V. J. & Rich, D. H., Eds., Pierce Chemical Co., Rockford, IL, pp. 477-486.
39. Bosch, R., Jung, G., Schmitt, H. & Winter, W. (1985) *Biopolymers* **24**, 961-978.
40. Bosch, R., Jung, G., Schmitt, H. & Winter, W. (1985) *Biopolymers* **24**, 979-999.
41. Karle, I. L., Sukumar, M. & Balamam, P. (1986) *Proc. Natl. Acad. Sci. USA* **83**, 9284-9288.
42. Karle, I. L., Flippen-Anderson, J. L., Sukumar, M. & Balamam, P. (1987) *Proc. Natl. Acad. Sci. USA* **84**, 5087-5091.
43. Rose, G. D., Gierasch, L. M. & Smith, J. A. (1985) *Adv. Protein Chem.* **37**, 1-109.
44. Das, M. K., Raghobama, S. & Balamam, P. (1986) *Biochemistry* **25**, 7110-7117.
45. Wüthrich, K., Billeter, M. & Braun, W. (1984) *J. Mol. Biol.* **180**, 715-740.
46. Shenderovich, M. D., Nikiforovich, G. V. & Chipens, G. I. (1984) *J. Magn. Reson.* **59**, 1-12.
47. Balamam, P., Bothner-By, A. A. & Dadok, J. (1972) *J. Am. Chem. Soc.* **94**, 4015-4016.
48. Ramachandran, G. N. & Sasisekharan, V. (1968) *Adv. Protein Chem.* **23**, 283-437.

Received June 24, 1987

Accepted November 2, 1987